J. Lundén, S. A. Kassam and V. Koivunen, "Robust nonparametric cyclic correlation based spectrum sensing for cognitive radio," *IEEE Transactions on Signal Processing*, 2009, to appear.

Robust Nonparametric Cyclic Correlation Based Spectrum Sensing for Cognitive Radio

Jarmo Lundén, Saleem A. Kassam, and Visa Koivunen

***Abstract*—Cognitive radios sense the radio spectrum in order to find underutilized spectrum and then exploit it in an agile manner. Spectrum sensing has to be performed reliably in challenging propagation environments characterized by shadowing and fading effects as well as heavy-tailed noise distributions. In this paper a robust computationally efficient nonparametric cyclic correlation estimator based on the multivariate (spatial) sign function is proposed. Nonparametric statistics provide additional robustness against heavy-tailed noise and when the noise statistics are not fully known. Asymptotic distribution of the spatial sign cyclic correlation estimator under the null hypothesis is established. Tests using constraint on false alarm rate are derived based on the estimated spatial sign cyclic correlation for single-user and collaborative spectrum sensing by multiple secondary users. Theoretical justification for detecting cyclostationary signals using the spatial sign cyclic correlation is provided. A sequential detection scheme for reducing the average detection time is proposed. Simulation experiments and theoretical results comparing the proposed method with cyclostationary spectrum sensing methods employing the conventional cyclic correlation estimator are presented. Simulations demonstrate the reliable and highly robust performance of the proposed nonparametric spectrum sensing method in both Gaussian and non-Gaussian noise environments.**

I. Introduction

Cognitive radio research has received considerable interest during the past few years. The interest in cognitive radios in wireless communications stems mainly from the scarcity of spectral resources [1]–[3]. Current spectrum regulation is based on a fixed frequency allocation policy. Each frequency band is allocated to a different wireless system in a rigid manner. This has resulted in an extremely uneven utilization of spectral resources both in time and space, thus, creating an increasing demand for more flexible and efficient utilization of spectral resources, demand for dynamic spectrum access. Dynamic spectrum access may be realized using cognitive radios. Cognitive radios sense the radio frequency spectrum for available spectral opportunities and utilize them in an intelligent manner. Spectrum sensing has to be performed reliably in the face of shadowing and fading effects as well as in difficult noise and interference environments. Collaborative sensing by multiple secondary users allows mitigation of shadowing and fading effects. Frequently changing noise and interference environments and associated statistical models call for robust approaches for spectrum sensing.

Robustness of spectrum sensing algorithms is motivated by several measurement studies that show the impulsive nature of man-made noise in many outdoor and indoor frequency bands [4]–[7]. Typical noise distribution according to these studies has heavier tails than normal distribution. Impulsive interference may be due to the presence of multiple interferers contaminating the primary signal we wish to detect. For example, indoor measurements in the industrial, scientific, and medical (ISM) bands reported in [5] show the impulsive nature of the noise and interference due to, e.g., microwave ovens and devices with electromechanical switches (electric motors in elevators, printers, copy machines, etc.) Moreover, on a computer platform various components, such as the LCD pixel clock and the PCI express bus, cause impulsive interference that degrades the performance of the embedded wireless devices [7], [8]. The impulsive interference on a computer platform is well modeled by a symmetric alpha-stable distribution [8]. As an example of outdoor measurements in urban environments, impulsive noise measurements in a digital television band (10 MHz bandwidth with a central frequency of 762 MHz) have been reported in [6]. Typical man-made impulsive noise sources in urban outdoor environments are igniting car engines, power lines, and heavy current switches. For more experimental measurement results demonstrating the impulsive nature of man-made noise, see [4]–[6], and the references therein.

Some of the most promising spectrum sensing algorithms exploit the cyclostationarity of wireless communication signals. Cyclostationary processes are stochastic processes whose statistical properties are periodic in time. Cyclostationarity in wireless communication signals may be caused by modulation or coding and may occur, for example, at the symbol rate or at the doubled carrier frequency. Cyclostationarity-based detection allows classifying signals exhibiting cyclostationarity at different cyclic frequencies. Hence, it has the potential to distinguish among primary users, secondary users, and interference, thus preparing the way for reliable and efficient co-existence of the primary and secondary users. Moreover, random noise commonly does not exhibit cyclostationarity.

Spectrum sensing algorithms exploiting cyclostationarity have been proposed, e.g., in [9]–[12]. The asymptotic distri-

The work has been done in collaboration with Nokia Research Center as part of the cognitive radio research.

Jarmo Lundén's work was further supported by GETA graduate school and Nokia Foundation.

J. Lundén and V. Koivunen are with the Department of Signal Processing and Acoustics, SMARAD CoE, Helsinki University of Technology, P. O. Box 3000, FI-02015 TKK, Finland, phone: +358 9 451 2398, fax: +358 9 452 3614, e-mail:{jrlunden,visa}@wooster.hut.fi.

S. A. Kassam is with the Department of Electrical and Systems Engineering, University of Pennsylvania, Philadelphia, PA 19104, USA, phone: +1 215 898 5990, fax: +1 215 573 2068, e-mail: kassam@ee.upenn.edu.

Some preliminary results of this work were presented in part at the 3nd Int. Conf. on Cognitive Radio Oriented Wireless Networks and Communications, Singapore, May 15–17, 2008.

butions of these detectors are based solely on the asymptotic distributions of the cyclic correlation estimators. That is, they do not require any explicit assumptions on the data or noise distributions. Nevertheless, these algorithms are not necessarily highly robust. For example, in case the noise distribution has heavier tails than normal distribution, the convergence of the sample estimator of the cyclic correlation slows down and the detection performance deteriorates.

Robust cyclic correlation estimators have been considered in [13] where estimators stemming from M-estimation are proposed. Both the proposed M-estimators as well as the trimmed mean estimator are found to reduce the influence of outliers (highly deviating observations). Simulation experiments demonstrate the significant improvement of performance of the robust estimators compared to the classical sample estimators in the face of non-Gaussian, heavy-tailed noise. However, M-estimators typically require estimation of nuisance parameters, such as the scale parameter. In addition, [13] focuses only on robust estimation of cyclic correlation without considering the detection of cyclostationary signals.

Cyclostationary detection in non-Gaussian noise has been considered in [14]. Single cycle and locally-optimum multicycle detectors are proposed. However, these detectors require the knowledge of the noise probability density function (pdf). Moreover, the multicycle detector requires the knowledge of the signal phase as well. The robust cyclostationary detectors proposed in this paper require only minimal assumptions on the noise pdf and do not require any assumptions on the signal phase.

The contributions of this paper are as follows. A cyclic correlation estimator based on the multivariate generalization of the sign function [16] applied to complex-valued data is proposed. It is shown that the cyclostationarity property used in the detector is preserved under the spatial sign function for an important special case, circularly symmetric complex normal distribution. Asymptotic distribution of the estimator under the null hypothesis is established. Test statistics for single-user and collaborative spectrum sensing schemes are proposed. A sequential detection scheme for reducing the average detection time is proposed as well. The asymptotic relative efficiency of the spatial sign cyclic correlation detector relative to the cyclic correlation detector of [10] is derived for complex normal input. Simulation experiments illustrating the robust performance of the proposed detectors in non-Gaussian noise environments as well as good performance in Gaussian noise environments are presented.

The proposed methods are based on nonparametric statistics making them highly attractive in real applications where noise and interference statistics may not be fully known or may change frequently. No additional nuisance parameters such as the scale need to be estimated unlike in the robust estimation methods in [13]. Furthermore, nonparametric detectors achieve a fixed false alarm rate under all conditions satisfying the nonparametric null hypothesis. In addition, the proposed detectors are computationally very efficient. The proposed detectors assume that at least one of the cyclic frequencies of the primary system is known. Such information is typically available since the primary user signals are specified in wireless standards and disclosure of such information is required by the regulatory bodies that allocate frequencies. Moreover, in order to be able to distinguish between primary users, secondary users, and interference, there has to be some prior knowledge about the primary users.

Introduction to main techniques of nonparametric signal detection has been given in [15]. Different multivariate sign and rank concepts, corresponding covariance matrices, and their statistical properties have been presented in [16]. Complex sign function employed in this paper can be considered to be the bivariate spatial sign function. Cyclic spectrum estimation algorithms based on correlating signal with its sign have been considered in [17] with the interest of reducing computational complexity. The signs of the real and imaginary parts are considered separately there.

This paper is organized as follows. Section II introduces the spatial sign cyclic correlation estimator. The asymptotic distribution of the estimator under the null hypothesis is established in Section III. In Section IV the testing problem is formulated as a hypothesis test, and the test statistics and their distributions under the null hypothesis are defined. In addition, a sequential detection scheme is proposed. In Section V the asymptotic relative efficiency of the spatial sign cyclic correlation detector relative to the cyclic correlation detector of [10] is established for complex normal input. Simulation experiments are presented in Section VI. Conclusion is given in Section VII. Theoretical results showing that the spatial sign function preserves the cyclostationarity of a circularly symmetric complex normal distributed stochastic process and the derivation of the asymptotic relative efficiency are provided in the Appendix.

II. Spatial Sign Cyclic Correlation

The spatial sign function for complex-valued data $x(t)$ is defined as [15], [16]

$$S(x(t)) = \begin{cases} \frac{x(t)}{|x(t)|}, & x(t) \neq 0 \\ 0, & x(t) = 0, \end{cases} \tag{1}$$

where $|\cdot|$ denotes the modulus of the complex-valued argument.

We define the spatial sign cyclic correlation estimator as

$$\hat{R}_S(\alpha, \tau) = \frac{1}{M} \sum_{t=0}^{M-1} S(x(t)) S(x^*(t+\tau)) e^{-j2\pi\alpha t}, \ \forall \tau \neq 0 \tag{2}$$

where $x(t)$ is a discrete time signal, τ is a discrete time delay, M is the number of observations and α is the cyclic frequency.

In (2) it has been assumed that the signal is centered, i.e. the mean of the data is zero. Otherwise an estimate for the mean using a robust estimator, such as the spatial median, has to be obtained and subtracted from the received signal before employing the estimator.

The use of the spatial sign function leads to an estimator that is both qualitatively and quantitatively robust, i.e. the effect of highly deviating samples is bounded and the method tolerates a high proportion of contaminated data. Qualitative robustness is verified by the influence function that has been

shown to be uniformly bounded for the spatial sign covariance estimator [18]. This result can be easily extended to spatial sign cyclic covariances at non-zero cyclic frequencies since a non-zero cyclic frequency adds only an exponential multiplier $e^{-j2\pi\alpha t}$ to the covariance estimator that does not affect the magnitude of the observation pairs. Hence, the influence function remains uniformly bounded.

An important consideration, especially from a practical point of view, is what is the effect of the spatial sign nonlinearity to the cyclic frequencies of the primary signal. In practice, this may have to be determined on a case by case basis either analytically or experimentally for each different primary user system. In the Appendix A it is shown that the periodicity of the autocorrelation function is preserved for a circularly symmetric complex Gaussian process in spite of the spatial sign function. For example, an orthogonal frequency division multiplexing (OFDM) signal is approximately normal distributed particularly when the number of subcarriers is sufficiently large. We will demonstrate that the spatial sign function preserves the cyclic frequencies of a cyclic prefix OFDM system with an example in the simulation experiments, as well. OFDM is employed in many existing and future wireless communications systems, such as the IEEE 802.11a/g wireless LANs, terrestrial digital television DVB-T, and 3GPP long term evolution, among others. Moreover, most of these systems employ sophisticated pilot structures that typically vary from system to system as well as between different modes (OFDM vs. OFDMA, TDD vs. FDD, SISO vs. MISO vs. MIMO, etc.). These pilot structures may induce strong cyclostationarity to the transmitted OFDM signal. This information may be exploited to improve the performance if the pilot-induced cyclic frequencies are known. However, here we focus on the cyclostationarity of the OFDM signal at the symbol frequency.

In order to define a test that satisfies a constraint on the false alarm rate for the presence of cyclostationarity at a given cyclic frequency, the distribution of the estimator needs to be established. In the next section, the distribution of the spatial sign cyclic correlation estimator is derived for independent and identically distributed (i.i.d.) circular noise process with zero mean. Nonparametric performance is achieved for all i.i.d. circular noise pdfs with zero mean. In practice, as already noted, if the mean is not zero it can be estimated and subtracted from the data. Note that circularity is not required from the primary user signal.

III. Distribution of the Spatial Sign Cyclic Correlation Estimator

In cognitive radio applications the number of observations M is typically large (in the order of several thousands). Consider, for example, the IEEE 802.22 standard draft for the opportunistic use of white space in digital television bands [19]. The channel bandwidths employed, for example, in the DVB-T (digital video broadcasting—terrestrial) standard are 6, 7, and 8 MHz [20]. Hence, Nyquist rate sampling for a millisecond would result in several thousands of observations. This allows us to apply the central limit theorem to infer the distribution of the spatial sign cyclic correlation estimator.

Central limit theorem for m-dependent variables states that the sum of m-dependent random variables with finite third absolute moment has a limiting normal distribution as the number of random variables goes to infinity [21]. A sequence of random variables are said to be m-dependent if any subset $(X_1, X_2, \ldots, X_r)$ is independent of any other subset $(X_s, X_{s+1}, \ldots)$ provided that $s-r > m$. The sequence of spatial sign correlation samples $S(x(t))S(x^*(t+\tau))$ formed from i.i.d. samples are m-dependent with $m = \tau$. Hence, according to the central limit theorem the distribution of the spatial sign cyclic correlation estimator approaches normal distribution as M goes to infinity. Thus, we can employ a normal distribution approximation for large M. Since a normal distribution is fully specified by its first and second order statistics, only the mean and covariance of the estimator need to be determined in order to fully specify the asymptotic distribution. Validity of the central limit theorem approximation will be assessed by simulations in Section VI.

We assume that $x(t) = n(t)$ where $n(t)$ is an i.i.d. circular noise process with zero mean. That is, only noise is considered to be present. In that case, the mean of $\hat{R}_S(\alpha, \tau)$ is given by ($\tau \neq 0$)

$$\begin{aligned} E[\hat{R}_S(\alpha,\tau)] &= \frac{1}{M}\sum_{t=0}^{M-1} E[S(n(t))S(n^*(t+\tau))]e^{-j2\pi\alpha t} \\ &= \frac{1}{M}\sum_{t=0}^{M-1} E[S(n(t))]E[S(n^*(t+\tau))]e^{-j2\pi\alpha t} \\ &= 0,\ \forall\alpha \end{aligned} \tag{3}$$

where the second equality follows from independence of the noise samples. The last equality follows from the fact that noise is assumed to be circular. Consequently, $S(n(t)) = e^{j\phi}$ where ϕ has a uniform distribution between 0 and 2π.

Since the mean is zero, the covariance of $\hat{R}_S(\alpha, \tau)$ and $\hat{R}_S(\beta, \rho)$ is given by ($\tau \neq 0, \rho \neq 0$)

$$\begin{aligned} &\mathrm{Cov}(\hat{R}_S(\alpha,\tau), \hat{R}_S^*(\beta,\rho)) = E[(\hat{R}_S(\alpha,\tau))(\hat{R}_S(\beta,\rho))^*] \\ &= E\left[\left(\frac{1}{M}\sum_{t=0}^{M-1} S(n(t))S(n^*(t+\tau))e^{-j2\pi\alpha t}\right)\right. \\ &\qquad \left.\cdot\left(\frac{1}{M}\sum_{k=0}^{M-1} S(n(k))S(n^*(k+\rho))e^{-j2\pi\beta k}\right)^*\right] \\ &= \frac{1}{M^2}\sum_{t=0}^{M-1}\sum_{k=0}^{M-1} E[S(n(t))S(n^*(k)) \\ &\qquad \cdot S(n^*(t+\tau))S(n(k+\rho)))]e^{-j2\pi(\alpha t-\beta k)} \\ &= \frac{1}{M^2}\left(\sum_{t=0}^{M-1} E[|S(n(t))|^2 S(n^*(t+\tau))S(n(t+\rho))]\right. \\ &\quad \cdot e^{-j2\pi(\alpha-\beta)t} + \sum_{t=0}^{M-1}\sum_{\substack{k=0\\k\neq t}}^{M-1} E[S(n(t))S(n^*(k)) \\ &\quad \left.\cdot S(n^*(t+\tau))S(n(k+\rho))]e^{-j2\pi(\alpha t-\beta k)}\right). \end{aligned} \tag{4}$$

Let us now consider the two sums separately. Since the noise process is i.i.d. and circular, the first sum is zero if $\tau \neq \rho$. When $\tau = \rho$, the expectation $E[|S(n(t))|^2|S(n(t+\tau))|^2] = 1$. Now let us consider the second sum. Since the noise process is i.i.d. and circular, the expectation can be non-zero only if $t = k+\rho$ and $k = t+\tau$, that is, when $\tau = -\rho$. However in that case, the expectation becomes $E[S(n(t))S(n^*(t+\tau))S(n^*(t+\tau))S(n(t))]$ which is zero as well since $n(t)$ is circular, and thus $E[S(n(t))S(n(t))] = 0, \forall t$. Consequently, the covariance of $\hat{R}_S(\alpha,\tau)$ for a circular i.i.d. process with zero mean is given by ($\tau \neq 0, \rho \neq 0$)

$$\begin{aligned}&\mathrm{Cov}(\hat{R}_S(\alpha,\tau), \hat{R}_S^*(\beta,\rho)) \\ &= \begin{cases} \frac{1}{M} & ,\alpha = \beta, \tau = \rho \neq 0, \\ \frac{1}{M^2}\sum_{t=0}^{M-1} e^{-j2\pi(\alpha-\beta)t} & ,\alpha \neq \beta, \tau = \rho \neq 0, \\ 0 & ,\tau \neq \rho. \end{cases}\end{aligned} \tag{5}$$

IV. Hypothesis Testing

We formulate the hypotheses as follows

$$\begin{aligned} H_0 &: x(t) = n(t), \\ H_1 &: x(t) = s(t) + n(t), \end{aligned} \tag{6}$$

where $x(t)$ is the received signal, $s(t)$ is the transmitted primary user signal that has possibly passed through a time-varying channel, and $n(t)$ is a circular i.i.d. noise process.

Under the null hypothesis H_0, the expected value of the estimated spatial sign cyclic correlation is zero. Under the alternative H_1, the expected value of the estimated spatial sign cyclic correlation is different from zero for the cyclic frequencies of the spatial sign of the primary user signal. Hence, we test whether the expected value of the estimated spatial sign cyclic correlation $\hat{R}_S(\alpha,\tau)$ is different from zero or not for one of the cyclic frequencies of the spatial sign of the primary user signal.

Let $\hat{\boldsymbol{r}}_S(\alpha)$ denote a vector that contains the estimated spatial sign cyclic correlations at cyclic frequency α for a set of time delays $\tau_1, \ldots, \tau_N$,

$$\hat{\boldsymbol{r}}_S(\alpha) = [\hat{R}_S(\alpha,\tau_1), \ldots, \hat{R}_S(\alpha,\tau_N)]^T. \tag{7}$$

From Section III, it follows that under the null hypothesis for large M

$$\hat{\boldsymbol{r}}_S(\alpha) \sim N_C(\boldsymbol{0}, \frac{1}{M}\boldsymbol{I}),\ \forall\alpha,\ \forall\tau_i \neq 0, i = 1, \ldots, N, \tag{8}$$

where $N_C(\cdot,\cdot)$ denotes the complex normal distribution and $\boldsymbol{I}$ the identity matrix.

Now, we define the test statistic for the spatial sign cyclic correlation based test for a single secondary user as

$$\lambda = M||\hat{\boldsymbol{r}}_S(\alpha)||^2, \tag{9}$$

where $||\cdot||$ denotes the Euclidean vector norm. Since the $\hat{R}_S(\alpha,\tau)$ are complex normal distributed, the test statistic λ is the log-likelihood under the null hypothesis after neglecting the constant terms. The null hypothesis is rejected if $\lambda > \gamma$ where γ is the test threshold defined by $p(\lambda > \gamma|H_0) = p_{fa}$. Here p_{fa} is the specified false alarm rate parameter of the test.

It follows that under the null hypothesis λ is asymptotically chi-square distributed with N complex degrees of freedom. The pdf of a chi-square distributed random variable with N complex degrees of freedom is given by

$$f(z) = \frac{1}{(N-1)!}z^{N-1}e^{-z},\ z > 0 \tag{10}$$

which is a gamma distribution with integer parameters N and 1. Consequently, the proposed test can be designed to satisfy a constraint on the false alarm rate. This property provides a rigorous way of allowing the secondary users to access the available spectrum on a regular basis when the primary user is not present. Excessive number of false alarms overwhelms the detectors and blocks the cognitive radio system from accessing the available spectrum, i.e., leads to overlooking spectral opportunities.

The proposed detector is a single cycle detector, i.e., it uses only one cyclic frequency of the primary user signal. However, wireless communication signals typically exhibit cyclostationarity at multiple cyclic frequencies. These cyclic frequencies may be related, for example, to symbol rate, coding and guard periods, and/or carrier frequency or their multiples. In order to take into account the rich information present in wireless communication signals, the proposed detector may be easily extended to multiple cyclic frequencies similarly to [11].

The proposed spatial sign cyclic correlation detector is computationally very efficient. Although there is the additional burden of the spatial sign computation, the benefit is that the covariance matrix of the estimator has a very simple form under the null hypothesis, depending only on the number of samples M. In addition, employing the spatial sign cyclic correlation estimator allows for straightforward sequential calculation of the test statistic as will be shown in the following section.

A. Sequential Detection

In this section a sequential detection scheme for single secondary users is proposed. Sequential detection aims at making decision without delay as soon as sufficiently reliable evidence for making decisions at specified error levels is available. The proposed sequential detection scheme employs a truncated test. That is, it is assumed that there is a maximum number of samples $M_{\max}$ that can be taken until a decision has to be made. A fairly recent review of classical problems, major developments, and future challenges in sequential analysis and detection is provided in [23].

Functional forms of the test statistic in (9) and the spatial sign cyclic correlation estimator in (2) allow for straightforward sequential calculation of the test statistic. That is, $\lambda(t) = \frac{1}{M_{\max}}||\hat{\boldsymbol{r}}_{S,t}(\alpha)||^2$ where the components of $\hat{\boldsymbol{r}}_{S,t}(\alpha)$ are calculated sequentially as follows

$$\hat{R}_{S,t}(\alpha,\tau) = \hat{R}_{S,t-1}(\alpha,\tau) + S(x(t))S(x^*(t+\tau))e^{-j2\pi\alpha t}, \tag{11}$$

for $t > 0$, and $\hat{R}_{S,0}(\alpha,\tau) = S(x(0))S(x^*(\tau))$.

The increments $S(x(t))S(x^*(t+\tau))e^{-j2\pi\alpha t}$ on the right-hand side of (11) are under H_0 i.i.d. samples drawn from a uniform distribution on the unit circle. Hence, $\hat{R}_{S,t}(\alpha,\tau)$ is a random walk in the complex plane (planar motion) with i.i.d. increments given by a uniform distribution on the unit circle.

Let us now denote the first time instant the absolute value of the random walk $Y(t) = \hat{R}_{S,t}(\alpha, \tau)$ exceeds value a by T_a, i.e.,

$$T_a = \inf\{t : |Y(t)| \geq a\}. \tag{12}$$

Now the probability that the absolute value of the random walk is equal to or above a at time t can be lower bounded by

$$\begin{aligned} p(|Y(t)| \geq a) &= p(|Y(t)| \geq a | T_a \leq t) p(T_a \leq t) \\ &\quad + \underbrace{p(|Y(t)| \geq a | T_a > t)}_{=0} p(T_a > t) \\ &= p(|Y(t)| \geq a | T_a \leq t) p(T_a \leq t) \\ &\geq \frac{1}{2} p(T_a \leq t) \end{aligned} \tag{13}$$

where the lower bound $p(|Y(t)| \geq a | T_a \leq t) \geq \frac{1}{2}$ follows from the fact that the probability that a random walk starting from outside or on the boundary of the disc of radius a returns inside the disc is less than or equal to $\frac{1}{2}$ due to the symmetry of the increment distribution.

It is easily shown (similarly as in (13)) that

$$p(T_a \leq t) = p(\max_{0 \leq s \leq t} |Y(s)| \geq a). \tag{14}$$

Hence, the probability of the maximum of the absolute value of the random walk Y between time instants 0 and t can be easily bounded by

$$p(|Y(t)| \geq a) \leq p(\max_{0 \leq s \leq t} |Y(s)| \geq a) \leq 2p(|Y(t)| \geq a), \tag{15}$$

where the lower bound follows trivially.

The above result allows us to define a truncated sequential detection test as follows

$$\begin{aligned} \text{If } \lambda(t) \geq \gamma_s \text{ and } t \leq M_{\max}, &\quad \text{Decide } H_1 \\ \text{If } \lambda(t) < \gamma_s \text{ and } t = M_{\max}, &\quad \text{Decide } H_0 \\ \text{Otherwise}, &\quad \text{Take a new sample, } t = t + 1, \end{aligned} \tag{16}$$

where $\lambda(t) = \frac{1}{M_{\max}} ||\hat{\boldsymbol{r}}_{S,t}(\alpha)||^2$, γ_s is the detection threshold, and $M_{\max}$ is the maximum number of samples that can be taken until a decision has to be made. Thus, only a decision to accept H_1 can be made before the maximum number of samples is reached. This strategy minimizes the probability of missed detection.

From (15) it follows that

$$p(\lambda(t) \geq \gamma_s) \leq p(\max_{0 \leq s \leq t} \lambda(s) \geq \gamma_s) \leq 2p(\lambda(t) \geq \gamma_s). \tag{17}$$

Hence, in order to constrain the false alarm rate, we can define the test threshold using the upper bound. That is, the test threshold is defined by $\beta = 2p(\lambda(M_{\max}) \geq \gamma_s | H_0)$ where β is the false alarm rate upper bound. Under the null hypothesis $\lambda(M_{\max})$ is asymptotically chi-square distributed with N complex degrees of freedom where N is the number of lags. Consequently, the test threshold can be easily set. The above threshold γ_s restricts the false alarm rate of the sequential detection test to remain in the interval $[\frac{1}{2}\beta, \beta]$.

B. Multiple Secondary Users

Secondary users have to perform spectrum sensing reliably in the face of shadowing and fading effects. These effects can be mitigated by exploiting spatial diversity through collaboration among secondary users. In this section, we propose collaborative tests for both the fixed sample size and the sequential test.

1) Fixed sample size test: Assuming that the test statistics of the secondary users are independent given H_0 or H_1, the single-user test statistics can be combined as follows

$$\lambda_L = \sum_{i=1}^{L} \lambda^{(i)} \tag{18}$$

where L is the number of collaborating secondary users and $\lambda^{(i)}$ denotes the spatial sign cyclic correlation test statistic of the ith user. Since the single-user test statistics $\lambda^{(i)}$ are the local log-likelihoods under the null hypothesis, the sum of the single-user test statistics in (18) follows assuming independence of the secondary user test statistics.

The sum of independent gamma (or chi-square) distributed random variables is also gamma (or chi-square) distributed where the shape parameter of the distribution of the sum is the sum of the shape parameters of the distributions of the individual random variables. Hence, under the null hypothesis λ_L is chi-square distributed with LN complex degrees of freedom (i.e., gamma distributed with parameters LN and 1).

2) Sequential detection: Since in sequential detection the decision is sought in shorter time, soft combining of the test statistics may result in performance loss. This is due to the fact that the secondary users will transmit their test statistics as soon as it exceeds the local test threshold. Hence, for the sequential detection test we employ a binary OR test at the fusion center (FC) (or at one of the secondary users when the network is operating in an ad-hoc manner without a dedicated FC). That is, each secondary user will send only their binary decision to the FC. The FC will accept H_1 if at least one of the secondary users has detected the primary user, i.e.,

$$\begin{aligned} \text{If } d_i = 1 \text{ for any } i = 1, \ldots, L, &\quad \text{Decide } H_1 \\ \text{Otherwise}, &\quad \text{Decide } H_0 \end{aligned} \tag{19}$$

where d_i is the decision of the secondary user i. That is, $d_i = 1$ if primary user is detected and otherwise $d_i = 0$.

Assuming independence of the secondary user test statistics under the null hypothesis, the false alarm rate at the FC is given by $\beta_{FC} = 1 - \prod_{i=1}^{L}(1 - \beta_i)$ where β_i are the false alarm rates of the secondary users. Hence, assuming identical false alarm rates for each secondary user, the local test thresholds of the secondary users can be defined by $\beta = 2p(\lambda(M_{\max}) \geq \gamma_s | H_0)$ where $\beta = 1 - (1 - \beta_{FC})^{1/L}$ is the false alarm rate upper bound of the local tests. The FC false alarm rate β_{FC} is bounded in the interval $[1 - (1 - \frac{1}{2}\beta)^L, 1 - (1 - \beta)^L]$.

V. Asymptotic Relative Efficiency

To obtain a theoretical indication of the performance loss due to the spatial sign non-linearity for a complex Gaussian distributed signal, such as the OFDM signal, in additive white Gaussian noise (AWGN) channel, we have derived the

asymptotic relative efficiency (ARE) of the spatial sign cyclic correlation detector relative to the cyclic correlation detector of [10] for a complex normal distributed input signal.

ARE is the ratio of the sample sizes of two tests of the same asymptotic size necessary to achieve the same asymptotic power against the same alternatives. That is, given tests A and B of asymptotic size α of the same hypotheses with equal asymptotic power $1-\beta$ ($\beta > 0$), and a sequence of alternatives $\{\theta_n\}$, the ARE of test A relative to test B is

$$ARE_{A,B} = \lim_{n\to\infty} \frac{m_{B,n}}{m_{A,n}}, \tag{20}$$

where $\{m_{A,n}\}$ and $\{m_{B,n}\}$ are the sequences of sample sizes of A and B, respectively.

The ARE of the spatial sign cyclic correlation detector relative to the cyclic correlation detector of [10] for weak signal detection for a complex normal input is given by (see Appendix B for derivation)

$$ARE = \frac{\pi^2}{16} \frac{\{\frac{1}{\sigma_c}\}\{\frac{1}{\sigma_c}\}^T}{\{\frac{1}{\sigma_c}\}\mathbf{\Lambda}^{-1}\{\frac{1}{\sigma_c}\}^T}, \tag{21}$$

where σ_c is the standard deviation of the cyclic correlation estimator of [10] and $\mathbf{\Lambda}$ is the normalized covariance matrix of the cyclic correlation estimates. Notation $\{\cdot\}$ denotes a matrix or a vector whose elements are given by the argument.

Assuming that the non-diagonal elements of $\mathbf{\Lambda}$ are zero, i.e. $\lambda_{ik} = 0, \forall i \neq k$, the ARE of the spatial sign cyclic correlation detector relative to the cyclic correlation detector of [10] for weak signal detection for a complex normal input is given by

$$ARE = \frac{\pi^2}{16} \approx 0.6169. \tag{22}$$

VI. Simulation Examples

In this section the performance of the proposed single cycle spatial sign cyclic correlation based detector is compared to the single cycle detectors proposed in [9]–[11] for both single and multiple secondary users. In [9], the optimum multicycle detector in Gaussian noise has been derived. However, the optimum multicycle detector cannot be implemented without the knowledge of the signal phase. The locally-optimum multicycle detector and the suboptimum single-cycle detector in non-Gaussian noise have been derived in [14]. However, they cannot be implemented without the knowledge of the noise pdf. Hence, we employ the suboptimum single-cycle detector (SCD) in Gaussian noise that correlates the ideal spectral correlation function (SCF) with the estimated SCF for one cyclic frequency of the signal. Consequently, it requires the knowledge of the ideal SCF, i.e., the knowledge of the modulation parameters such as the carrier frequency, pulse shape, and symbol frequency. We extend the SCD to multiple secondary users by taking the sum over the local test statistics at the FC. The asymptotic distributions of the SCD have been established in [26], [27]. In [10], generalized likelihood ratio tests for the presence of cyclostationarity have been proposed. We employ the 2nd-order time domain test for the cyclic frequency in question, i.e., for example, the symbol frequency. Hence, the knowledge of the symbol frequency is required. In [11] the time domain test has been extended to collaborative detection by calculating the sum over the local test statistics of the secondary users. The cyclic spectrum values required for the covariance matrix were estimated using a frequency-smoothed cyclic periodogram with length 2049 Kaiser window with β parameter of 10. We denote this test by the abbreviation STPC (statistical test for the presence of cyclostationarity). In addition, we employ the STPC detector for the observations that have been passed through the Huber function nonlinearity proposed in [13] for robust cyclic correlation estimation. The Huber ψ function is given by $\psi(x) = x$, for $|x| < a$, and $\psi(x) = ax/|x|$, otherwise. The scale is estimated using the complex median of the absolute deviations from the median (CMAD) [13] and Huber function threshold parameter $a = 1$ is employed. This detector is denoted by STPC Huber.

However, we begin by illustrating with an example that the spatial sign non-linearity preserves the cyclic frequencies due to the symbol frequency for a cyclic prefix OFDM signal. Fig. 1 shows the normalized squared modulus of the cyclic correlation for a cyclic prefix OFDM signal for the conventional and spatial sign estimators. It can be seen that the cyclic frequencies are preserved by the spatial sign non-linearity. Note that in practice the magnitudes of the cyclic correlation and spatial cyclic correlation are different. Magnitudes have been normalized here for easier comparison.

Secondly, we consider the validity of the central limit theorem approximation of the spatial sign cyclic correlation estimator by considering the distribution of the spatial sign cyclic correlation based test statistic. Fig. 2 plots the probability density and cumulative distribution functions of the test statistic $\lambda = M||\hat{\boldsymbol{r}}_S(\alpha)||^2$ for a circularly symmetric i.i.d. contaminated complex Gaussian process $0.95N_C(0,\sigma^2) + 0.05N_C(0,25\sigma^2)$. That is, with a probability of 0.95 the noise comes from the first distribution $N_C(0,\sigma^2)$ and with a probability of 0.05 from the second $N_C(0,25\sigma^2)$. The number of observations $M = 100$. Two random lags between 1 and 20 observations and a random cyclic frequency in the interval $[0.05, 0.5]$ were employed. The histogram and empirical cumulative distribution functions have been obtained from 10000 experiments. The measured empirical distribution is very accurately approximated by the derived theoretical distribution thus confirming the validity of the central limit theorem approximation.

The first test signal is an OFDM signal. The employed OFDM signal is a DVB-T signal with a fast-Fourier transform (FFT) size $N_{FFT} = 8192$ and a cyclic prefix of $N_{cp} = 1024$ samples. The symbol length is given by $N_{FFT} + N_{cp}$. The number of employed subcarriers is 6817, the subcarrier modulation is 64-QAM (quadrature amplitude modulation), and the length of the signal is 3 OFDM symbols ($\approx$ 3 ms). The signal was sampled at the Nyquist rate. Thus, the oversampling factor with respect to the symbol rate is $N_{FFT} + N_{cp}$.

Cyclic prefix OFDM signal is cyclostationary with respect to the symbol frequency. Thus, the detection is performed at the symbol frequency by all detectors. In addition, all the detectors except SCD, which takes the weighted sum over all time delays, employ two time lags $\pm N_{FFT}$. The cyclic autocorrelation of the OFDM signal peaks for these time

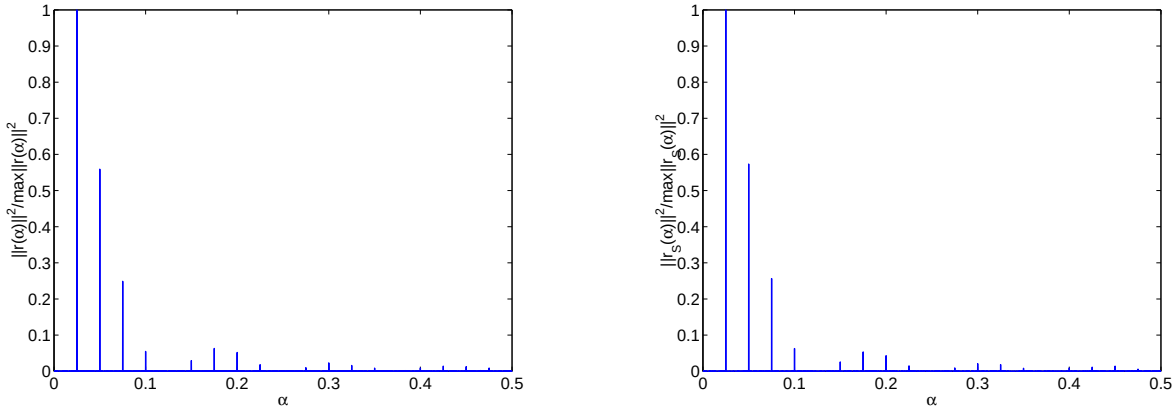

(a) Cyclic correlation

(b) Spatial sign cyclic correlation

Figure 1. Normalized squared modulus of (a) the cyclic correlation, and (b) the spatial sign cyclic correlation. The signal is a cyclic prefix OFDM signal with symbol frequency of 0.025. The spatial sign non-linearity preserves the cyclic frequencies.

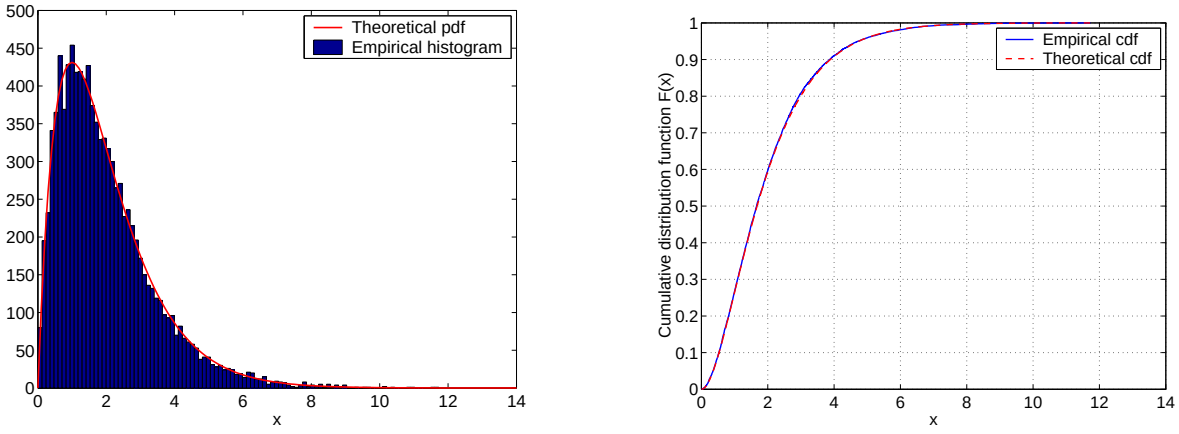

(a) Probability density function

(b) Cumulative distribution function

Figure 2. Validity of the central limit theorem approximation for the spatial sign cyclic correlation estimator. (a) Probability density function and (b) cumulative distribution function of the test statistic $\lambda = M||\hat{\boldsymbol{r}}_S(\alpha)||^2$ for a contaminated Gaussian process $0.95N_C(0,\sigma^2) + 0.05N_C(0,25\sigma^2)$. The number of observations $M = 100$. The measured empirical distribution is very accurately approximated by the distribution derived using the central limit theorem.

lags [28].

Fig. 3 plots the performance of the detectors for 1 and 5 secondary users in AWGN channel as a function of the signal-to-noise ratio (SNR). The SNR is defined as $\mathrm{SNR} = 10\log_{10}\frac{\sigma_x^2}{\sigma_n^2}$ where σ_x^2 and σ_n^2 are the variances of the transmitted signal and the noise, respectively. False alarm rate is set to 0.05. The same false alarm rate is employed throughout the simulations. All the simulation curves in the figures are averages over 1000 independent experiments.

It can be seen that employing the spatial sign non-linearity causes performance degradation in AWGN channel compared to the SCD and STPC detectors. The SCD detector has the best performance as expected since it employs more prior knowledge than the other detectors. However, this makes it also more susceptible to synchronization errors. Unlike the other detectors, the SCD requires the knowledge of the carrier frequency, thus requiring carrier frequency estimation. In the simulation the carrier frequency was assumed to be known. The STPC Huber detector has very similar but slightly worse performance than the spatial sign detector (the curves are almost overlapping). However, its computational complexity is much higher than the spatial sign detector's complexity since it requires the estimation of the covariance matrix due to the use of the STPC detector. Moreover, it requires estimation of the scale parameter. For the sake of clarity, in the following OFDM simulations we will omit the performance curve of the STPC Huber detector since it is very close to the performance of the spatial sign cyclic correlation detector.

Fig. 4 depicts the performance of the detectors in a contaminated Gaussian distribution. The contaminated Gaussian distribution is $0.95N_C(0,\sigma^2) + 0.05N_C(0,100\sigma^2)$. This can be interpreted as that there is 5 % probability at each time instant that noise is more impulsive and comes from a distribution with significantly higher variance. The contaminated Gaussian noise model has been shown to provide a very good approximation to the Middleton Class A noise model in many different measurements [29]. Moreover, the Middleton Class A noise model has been shown to provide an accurate fit to experimental data in a variety of different measurements [4]. The typical parameter values of the contaminated Gaussian distribution derived from the measurements and approximation to the Middleton Class A noise model are in the range

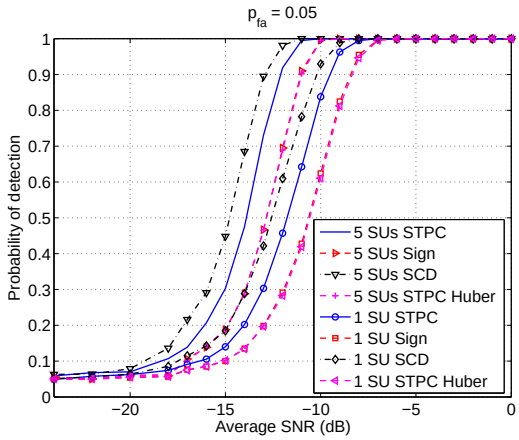

Figure 3. Probability of detection vs. SNR (dB) in an AWGN channel for 1 and 5 secondary users (SUs). The signal is an OFDM signal (DVB-T). Spatial sign cyclic correlation based detector suffers small performance degradation compared to the methods based on conventional cyclic correlation estimator in Gaussian noise for the OFDM signal.

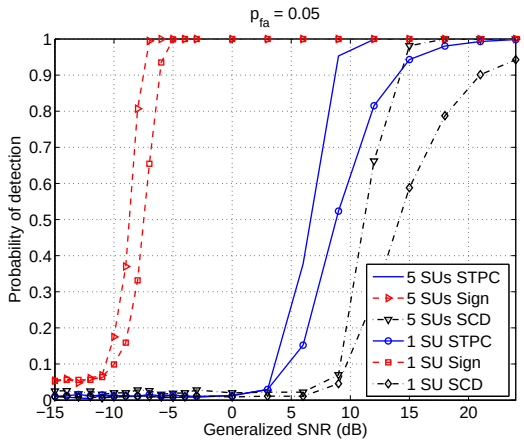

Figure 5. Probability of detection vs. Generalized SNR (dB) in an additive complex isotropic Cauchy noise channel for 1 and 5 secondary users. The signal is an OFDM signal (DVB-T). The spatial sign cyclic correlation based detector is more robust against the heavy-tailed Cauchy noise than the other detectors.

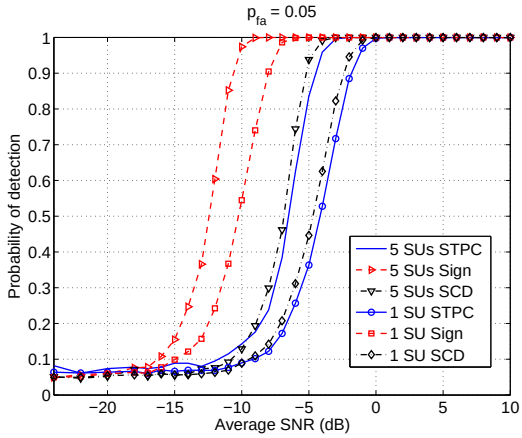

Figure 4. Probability of detection vs. SNR (dB) in a contaminated additive Gaussian noise channel for 1 and 5 secondary users. Additive noise has a contaminated Gaussian distribution $0.95N_C(0,\sigma^2) + 0.05N_C(0,100\sigma^2)$. SNR is defined with respect to σ^2. The signal is an OFDM signal (DVB-T). The spatial sign cyclic correlation based detector is more robust against impulsive non-Gaussian noise than the other detectors.

$\epsilon = [0.01,\ 0.33]$ and $\sigma_1^2/\sigma_0^2 = [20,\ 10000]$ where ϵ is the probability of the impulsive component and σ_1^2/σ_0^2 is the ratio of the variances of the two Gaussian component distributions [24], [29].

The robustness of the spatial sign cyclic correlation based detector compared to the STPC detector and the SCD is clearly evident in the contaminated Gaussian noise case.

Fig. 5 depicts the performance of the detectors in additive complex isotropic Cauchy distributed noise to demonstrate the highly robust performance of the proposed detectors. The noise location parameter is zero (because the mean is not defined for the Cauchy distribution). The Cauchy distribution is a heavy-tailed alpha-stable distribution whose variance is undefined and second moment is infinite. In fact both the Gaussian and Cauchy distributions are special cases of the symmetric alpha-stable distributions. The relationship of the symmetric alpha-stable distribution to the Middleton Class B noise model has been considered in [30]. Moreover, it is shown with a large variety of different real data that the symmetric alpha-stable noise model provides a similar accurate fit to real data as the Middleton Class B noise model.

The performances are defined as a function of the generalized SNR (GSNR). The GSNR is defined as $\mathrm{GSNR} = 10\log_{10}\frac{\sigma_x^2}{\gamma}$ where σ_x^2 is the variance of the transmitted signal and γ is the dispersion of the Cauchy noise. The spatial sign cyclic correlation based detector is significantly more robust against the heavy-tailed Cauchy noise than the other detectors.

Rayleigh fading causes an additional loss in performance as demonstrated by Fig. 6 that depicts the performance of the detectors in a Rayleigh fading channel (ETSI EN 300 744 V1.5.1 (2004-11) [20]) and AWGN as a function of the average SNR. The channel is normalized to have an expected gain of 1. The loss in performance due to fading is similar to all detectors. Collaborative detection curves show that fading effects can be mitigated by collaboration among secondary users.

Fig. 7 shows the performances in the same Rayleigh fading channel for the DVB-T signal in a heavy-tailed noise environment. The noise has a complex isotropic Cauchy distribution. The robustness of the nonparametric spatial sign cyclic correlation based detector compared to the STPC detector and the SCD can be clearly seen.

In [8], the symmetric alpha-stable distribution with $\alpha = 1.4329$ was found to provide a good match to measurement data of the radio frequency interference experienced in embedded laptop wireless receivers. The non-Gaussian impulsive interference due to the internal components, for example in the ISM band at 2.4 GHz, is caused mainly by the LCD pixel clock harmonics [7]. Other possible sources of interference on a computer platform are, for example, the gigabit ethernet and PCI express bus [8]. Fig. 8 depicts the performance of the cyclic detectors in complex isotropic alpha-stable noise channel with $\alpha = 1.4329$ for 1 and 5 secondary users for an IEEE 802.11 WLAN (wireless local area network) OFDM

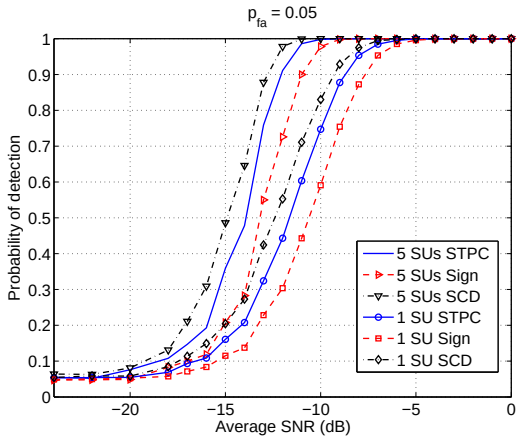

Figure 6. Probability of detection vs. Average SNR (dB) in a Rayleigh fading channel for 1 and 5 secondary users. The additive noise is Gaussian. The signal is an OFDM signal (DVB-T). Rayleigh fading degrades the performance for single-user detection. However, collaboration among the secondary users allows mitigation of fading effects.

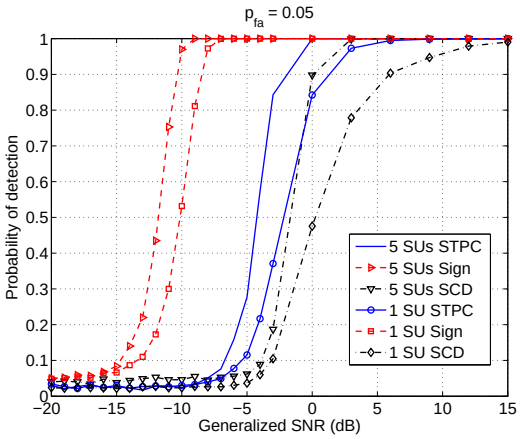

Figure 8. Probability of detection vs. Generalized SNR (dB) in an additive complex isotropic alpha-stable noise channel with $\alpha = 1.4329$ for 1 and 5 secondary users. The signal is a WLAN OFDM signal. The spatial sign cyclic correlation based detector is more robust against the heavy-tailed alpha-stable noise than the other detectors.

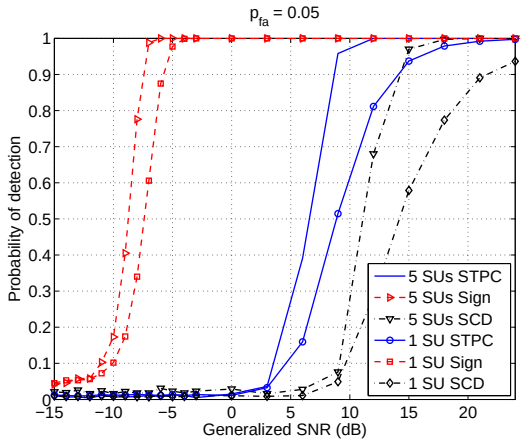

Figure 7. Probability of detection vs. Generalized SNR (dB) in a Rayleigh fading channel for 1 and 5 secondary users. Additive noise has a complex isotropic Cauchy distribution. The signal is an OFDM signal (DVB-T). The spatial sign cyclic correlation based detector is more robust against heavy-tailed noise also in a Rayleigh fading channel.

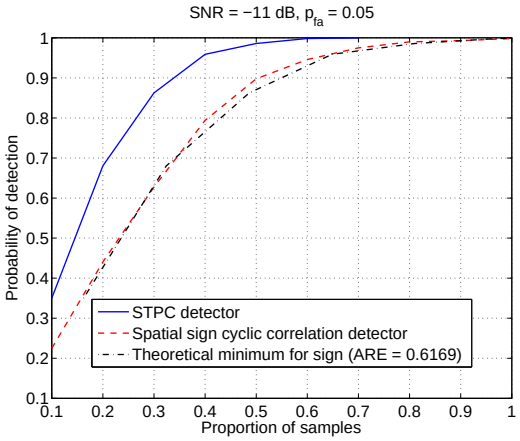

Figure 9. Probability of detection vs. Proportion of samples in AWGN channel at SNR of -11 dB. The signal is an OFDM signal (WLAN). The maximum signal length is 2 ms. Theoretical performance curve for the spatial sign cyclic correlation detector has been obtained from the performance curve of the STPC detector by dividing its corresponding sample sizes with the theoretical ARE $\pi^2/16 \approx 0.6169$.

signal. The size of the FFT $N_{FFT} = 64$, the number of occupied subcarriers is 52, the cyclic prefix $N_{cp} = 16$ samples, and the subcarrier modulation is quadrature phase shift keying (QPSK). The signal length is 1 ms. The proposed spatial sign cyclic correlation based detector has very robust performance. The performance difference to the STPC detector is roughly 7 dB and to the SCD roughly 10 dB.

OFDM signal is well approximated by normal distribution especially when the number of subcarriers is sufficiently large. Hence, we can use OFDM signals to evaluate numerically the derived theoretical result for the ARE of the spatial sign cyclic correlation detector relative to the cyclic correlation detector.

Fig. 9 depicts the performance of the spatial sign cyclic correlation detector relative to the cyclic correlation detector of [10] as a function of the signal length in AWGN at SNR of -11 dB. The signal is an IEEE 802.11 WLAN OFDM signal. The signal parameters are the same as in Fig. 8. The maximum signal length is 2 ms. The results suggest that the theoretical analysis of the ARE is indicative of realistic performance for cyclostationary signals. The correlation function of the employed noise free OFDM signal is unity at the cyclic prefix (20% of the time) and zero otherwise (80% of the time) for the time lags $\pm N_{FFT}$. Hence, it is cyclostationary with a period of $N_{FFT} + N_{cp}$ samples.

The second test signal is a QPSK signal with root raised-cosine pulse shaping with excess bandwidth of 0.2. The length of the signal is 1500 symbols. The signal was four times oversampled. Detection was performed at the symbol frequency. The spatial sign detector employed the time delays $\pm 1, \pm 2, \ldots, \pm 5$ samples. The STPC detectors employed the same time delays as the spatial sign detector as well as the time delay 0.

Figs. 10 and 11 depict the performances of the detectors for the QPSK signal in a frequency flat Rayleigh fading channel for Gaussian and Cauchy noise distributions, respectively. In

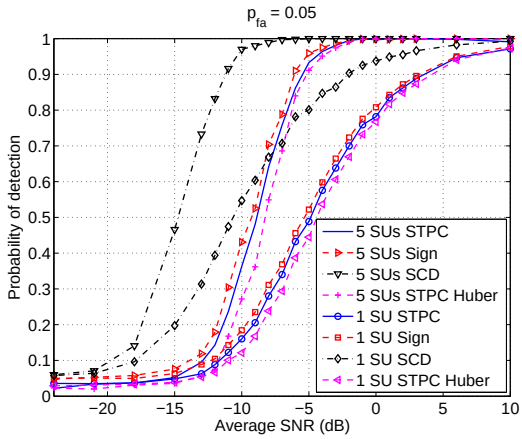

Figure 10. Probability of detection vs. Average SNR (dB) in a frequency flat Rayleigh fading channel for 1 and 5 secondary users. Additive noise is Gaussian. Signal is a QPSK signal with root raised-cosine pulse shaping. The nonparametric spatial sign cyclic correlation based detectors slightly outperform the STPC detectors even in Gaussian noise for the QPSK signal.

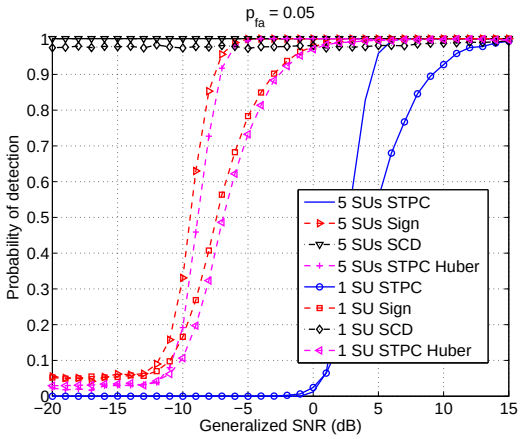

Figure 11. Probability of detection vs. Generalized SNR (dB) in a frequency flat Rayleigh fading channel for 1 and 5 secondary users. Additive noise is Cauchy distributed. Signal is a QPSK signal with root raised-cosine pulse shaping. Due to the heavy-tailed nature of the noise the robust spatial sign cyclic correlation based detector clearly outperforms the methods based on the conventional cyclic correlation estimator. The SCD breaks down and results in a false alarm rate over 0.95.

this case, the spatial sign cyclic correlation detector slightly outperforms the STPC detector even in the non-impulsive noise environment. Unlike the spatial sign cyclic correlation based detector, the conventional cyclic detector requires estimation of the covariance matrix of the estimator. This can be considered as a nuisance parameter whose estimation may result in a small performance loss, especially, for small number of observations. This is further illustrated by the STPC Huber detector that has roughly 1 dB worse performance than the spatial sign detector. The SCD has clearly the best performance in the Gaussian noise. However, the SCD is not robust and breaks down in the Cauchy noise, thus having a false alarm rate over 0.95. In the heavy-tailed noise environment the robustness of the spatial sign cyclic correlation based detector is clearly evident. This is further illustrated in Fig. 12 where the performance curves are plotted for different heavy-tailed non-Gaussian noise environments. The heavier the tails of the noise distribution are, the larger is the performance difference between the spatial sign cyclic correlation and the STPC detector of [10].

Fig. 13 depicts the performance of the sequential and fixed sample size spatial sign detector as a function of the SNR. The channel is a frequency flat Rayleigh fading channel. The signal is an IEEE 802.11 WLAN OFDM signal. The size of the FFT $N_{FFT} = 64$, the number of occupied subcarriers is 52, the cyclic prefix $N_{cp} = 16$ samples, and the subcarrier modulation is QPSK. The maximum sensing time for the sequential detectors and also used by the fixed sample size detectors is 3 ms. The sequential detectors have comparable performance to the fixed sample size spatial sign cyclic correlation detectors. Note that for the sequential detectors the upper bound of the false alarm rate is 0.05.

Fig. 14 plots the average proportion of samples required to make a decision for the sequential detectors as a function of the SNR. The FC test refers to the minimum sensing time of the secondary users. Sequential detection schemes provide considerable reduction in the detection times.

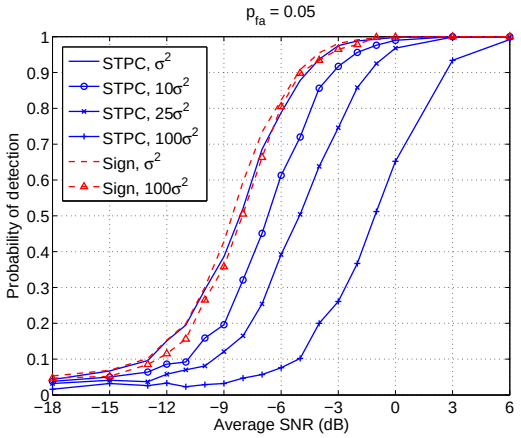

Figure 12. Probability of detection vs. Average SNR (dB) in a frequency flat Rayleigh fading channel for 5 secondary users in different noise environments. Additive noise has a contaminated Gaussian distribution $0.95N_C(0, \sigma^2) + 0.05N_C(0, \sigma_i^2)$ where $\sigma_i^2 \in [\sigma^2, 10\sigma^2, 25\sigma^2, 100\sigma^2]$. SNR is defined with respect to σ^2. Signal is a QPSK signal with root raised-cosine pulse shaping. For the sake of clarity, the $10\sigma^2$- and $25\sigma^2$-curves for the spatial sign detector have not been plotted. They position between the σ^2- and $100\sigma^2$-curves for the spatial sign detector. The heavier the tails of the noise distribution, the larger the performance difference between the spatial sign cyclic correlation and the STPC detector of [10].

VII. Conclusion

In this paper a nonparametric spatial sign cyclic correlation based spectrum sensing method for cognitive radio systems has been proposed. It has been shown that the spatial sign cyclic correlation function remains periodic for circularly symmetric complex normal processes. Asymptotic distributions of the test statistics under the null hypothesis have been derived. Tests for single-user and collaborative detection have been developed. The ARE of the spatial sign cyclic correlation detector relative to the cyclic correlation detector of [10] for complex Gaussian inputs has been derived. For the complex Gaussian case the efficacy of the spatial sign cyclic correlation detector is 61.7 % of the efficacy of the cyclic correlation detector of [10],

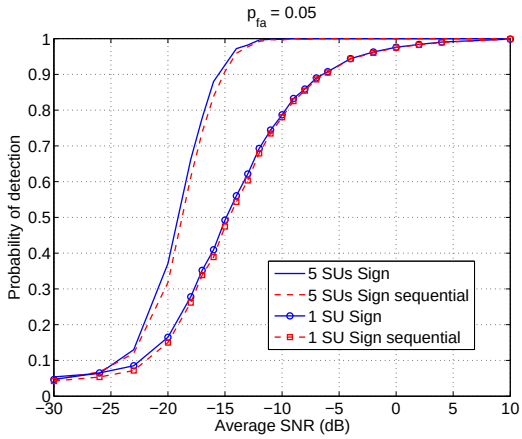

Figure 13. Probability of detection vs. Average SNR (dB) in a frequency flat Rayleigh fading channel for 1 and 5 secondary users. Additive noise has a Gaussian distribution. The signal is an OFDM signal (WLAN). The maximum sensing time is 3 ms. The sequential detection scheme provides comparable performance to the fixed sample size spatial sign cyclic correlation detector.

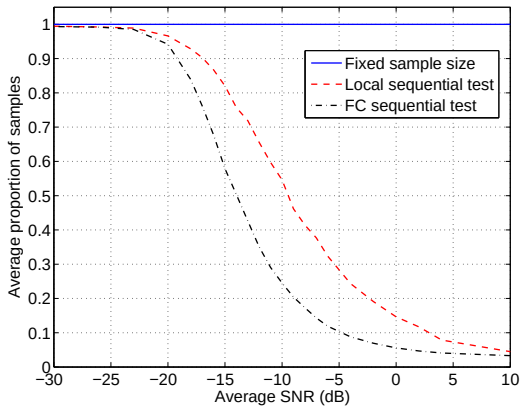

Figure 14. Average proportion of samples used vs. Average SNR (dB) in a frequency flat Rayleigh fading channel for local and FC tests for a cooperation of 5 users. Additive noise has a Gaussian distribution. The signal is an OFDM signal (WLAN). The maximum sensing time is 3 ms. The sequential detection scheme reduces the required number of samples significantly compared to the fixed sample size spatial sign cyclic correlation detector with approximately equal performance.

resulting in a 1 dB performance loss for the DVB-T OFDM signal in additive white Gaussian noise. However, significant benefits for the non-Gaussian cases are obtained: 2–15 dB performance gain depending on the heaviness of the tails of the noise distribution have been observed for the OFDM and QPSK signals in non-Gaussian heavy-tailed noise compared to the cyclic correlation detector of [10]. The performance of the proposed spatial sign cyclic detector has been compared to the SCD [9] and a robust detector based on [10] and the Huber function as well. The SCD has been seen to perform best in Gaussian noise. However, it requires more prior knowledge than the other detectors and has been seen not to be robust in heavy-tailed noise. The considered robust Huber function based cyclic detector has almost as good performance as the proposed spatial sign cyclic detector, however, it has much higher computational complexity.

Finally, in addition to the fixed sample size detector, a sequential spatial sign cyclic correlation based detection scheme has been proposed. The sequential detection scheme has been seen to provide shorter detection time on average than the fixed sample size detector with roughly equal performance.

APPENDIX

A. Cyclostationarity of the Spatial Sign of a Complex Gaussian Process

Considering the effects of the spatial sign non-linearity for a general cyclostationary process is not an easy task. However, certain results that apply for high SNR cases can be defined for special type of inputs. Here, we will consider a complex Gaussian input process. Although many of the communication signals may not be Gaussian, the Gaussian process is still a very important special case. For example, an OFDM signal is well approximated by a Gaussian process for a sufficiently large number of subcarriers.

Assume that the input signal to the hard-limiting spatial sign non-linearity is a zero-mean circularly symmetric complex Gaussian process. Then it follows that the normalized complex autocorrelation function of the hard-limited process $y(t) = S(x(t))$ is given by [31], [32]

$$\begin{aligned}\rho_{yy}(t,\tau) &= E[S(x(t))S^*(x(t+\tau))] \\ &= \frac{\pi}{4}\rho_{xx}(t,\tau)\ {}_2F_1\left(\frac{1}{2},\frac{1}{2};2;|\rho_{xx}(t,\tau)|^2\right),\end{aligned} \tag{23}$$

where $\rho_{xx}(t,\tau)$ is the normalized autocorrelation function of $x(t)$, i.e., $\rho_{xx}(t,\tau) = \frac{E[x(t)x^*(t+\tau)]}{\sqrt{E[x(t)x^*(t)]E[x(t+\tau)x^*(t+\tau)]}}$. ${}_2F_1(\cdot,\cdot;\cdot;\cdot)$ is the Gaussian hypergeometric function given by the following series representation

$$\begin{aligned}{}_2F_1\left(\frac{1}{2},\frac{1}{2};2;|\rho|^2\right) &= \frac{\Gamma(2)}{\Gamma^2(\frac{1}{2})}\sum_{n=0}^{\infty}\frac{\Gamma^2(\frac{1}{2}+n)}{\Gamma(2+n)}\frac{|\rho|^{2n}}{n!} \\ &= 1+\frac{1}{8}|\rho|^2+\frac{3}{64}|\rho|^4+\frac{25}{1024}|\rho|^6+\ldots\end{aligned} \tag{24}$$

From (23) it can be seen that the phase of the autocorrelation function is unaltered by the spatial sign non-linearity. Furthermore, we can make the following approximations: $\rho_{yy}(t,\tau) \approx \rho_{xx}(t,\tau)$ when $|\rho_{xx}(t,\tau)|$ is close to unity, and $\rho_{yy}(t,\tau) \approx \frac{\pi}{4}\rho_{xx}(t,\tau)$ when $|\rho_{xx}(t,\tau)|$ is close to zero.

Hence, the periodicity of the autocorrelation function of a circularly symmetric complex Gaussian process is preserved by the spatial sign non-linearity (although the autocorrelation may be attenuated). Note, however, that in principle the spatial non-linearity may also cause periodicities that do not exist in the original autocorrelation function due to the second and higher terms in (24). Higher-order statistics of cyclostationary signals have been discussed in [22] and the references therein.

B. Asymptotic Relative Efficiency

In order to obtain the asymptotic power of a test, we consider testing the null hypothesis H_0 against a sequence of alternatives H_n

$$\begin{aligned}H_0 &: \theta = 0, \\ H_n &: \theta = \gamma/\sqrt{n},\end{aligned}$$

where γ is an arbitrary positive constant. This formulation is especially appropriate for weak signal detection. The derived ARE will correspond to a situation when the sequence of alternatives approaches the null hypothesis, that is, to very low SNR regimes. We can calculate the ARE of two sequences of detectors for the above hypothesis testing problem as follows.

Let $\{D_{A,n}\}$ and $\{D_{B,n}\}$ be two sequences of detectors based on corresponding sequences of test statistics $\{\boldsymbol{T}_{A,n}(\boldsymbol{X})\}$ and $\{\boldsymbol{T}_{B,n}(\boldsymbol{X})\}$ of dimension K, respectively. Let both detector sequences be of asymptotic size α, let $\boldsymbol{\mu}_{A,n}(\theta)$ and $\boldsymbol{\mu}_{B,n}(\theta)$ be the mean, and $\boldsymbol{\sigma}^2_{A,n}(\theta)$ and $\boldsymbol{\sigma}^2_{B,n}(\theta)$ be the variance vectors of the test statistics $\{\boldsymbol{T}_{A,n}(\boldsymbol{X})\}$ and $\{\boldsymbol{T}_{B,n}(\boldsymbol{X})\}$ for $\theta \geq 0$, respectively. Let the covariances for $\theta \geq 0$ be $\sigma_{A,kn}(\theta)\sigma_{A,in}(\theta)\lambda_{A,ikn}(\theta)$ and $\sigma_{B,kn}(\theta)\sigma_{B,in}(\theta)\lambda_{B,ikn}(\theta)$ where $\lambda_{A,ikn}(\theta)$ and $\lambda_{B,ikn}(\theta)$ are the normalized covariances of $T_{A,kn}(\boldsymbol{X})$ and $T_{A,in}(\boldsymbol{X})$, and $T_{B,kn}(\boldsymbol{X})$ and $T_{B,in}(\boldsymbol{X})$, $k = 1, 2, \ldots, K$, and $i = 1, 2, \ldots, K$, respectively. If both sequences of test statistics satisfy the following regularity conditions [24]:

$$\text{(i)}\ \frac{d}{d\theta}\mu_{kn}(\theta)\Big|_{\theta=0} = \mu'_{kn}(0) > 0, \text{ for } k = 1, 2, \ldots, K, \quad (25)$$

$$\text{(ii)}\ \lim_{n\to\infty} \frac{\mu'_{kn}(0)}{\sqrt{n}\sigma_{kn}(0)} = c_k > 0, \text{ for } k = 1, 2, \ldots, K, \quad (26)$$

$$\text{(iii) For } \theta_n = \gamma/\sqrt{n}, \text{ with } \gamma \geq 0,$$
$$\lim_{n\to\infty} \frac{\mu'_{kn}(\theta_n)}{\mu'_{kn}(0)} = \lim_{n\to\infty} \frac{\sigma_{kn}(\theta_n)}{\sigma_{kn}(0)} = \lim_{n\to\infty} \frac{\lambda_{ikn}(\theta_n)}{\lambda_{ikn}(0)} = 1,$$
$$\text{for } k = 1, 2, \ldots, K;\ i = 1, 2, \ldots, K, \quad (27)$$

$$\text{(iv) } [T_{kn}(\boldsymbol{X}) - \mu_{kn}(\theta_n)]/\sigma_{kn}(\theta_n), \text{ for } k = 1, 2, \ldots, K,$$
$$\text{have asymptotically a multivariate normal distribution,} \quad (28)$$

then the ARE of $\{D_{A,n}\}$ with respect to $\{D_{B,n}\}$ is

$$ARE_{A,B} = \frac{\xi_A}{\xi_B} \quad (29)$$

where ξ_A and ξ_B are the efficacies of D_A and D_B, respectively. Efficacy is a measure of efficiency for one test. The efficacy of the test statistic $T_{kn}(\boldsymbol{X})$ is defined as

$$\xi = \lim_{n\to\infty} \left[\frac{\mu'_{kn}(0)}{\sqrt{n}\sigma_{kn}(0)}\right]^2. \quad (30)$$

For two chi-square distributed test statistics of the form

$$Q_n = \boldsymbol{q}_n(\theta)\boldsymbol{\Lambda}_n^{-1}(\theta)\boldsymbol{q}_n(\theta)^T, \quad (31)$$

where the elements of $\boldsymbol{q}_n(\theta)$ are $q_{kn}(\theta) = [T_{kn}(\boldsymbol{X}) - \mu_{kn}(\theta)]/\sigma_{kn}(\theta)$, $k = 1, \ldots, K$, and $\boldsymbol{\Lambda}_n(\theta) = \{\lambda_{ikn}(\theta)\}$ ($\{\cdot\}$ denotes a matrix whose elements are given by the argument), the ARE for the same sequence of alternatives is the ratio of the respective non-centrality parameters of the distributions of the test statistics under H_n, i.e., [24], [25]

$$ARE_{A,B} = \frac{\gamma^2 \boldsymbol{c}_A \boldsymbol{\Lambda}_A^{-1}(0)\boldsymbol{c}_A^T}{\gamma^2 \boldsymbol{c}_B \boldsymbol{\Lambda}_B^{-1}(0)\boldsymbol{c}_B^T} = \frac{\boldsymbol{c}_A \boldsymbol{\Lambda}_A^{-1}(0)\boldsymbol{c}_A^T}{\boldsymbol{c}_B \boldsymbol{\Lambda}_B^{-1}(0)\boldsymbol{c}_B^T}, \quad (32)$$

where $\boldsymbol{c}_A = [c_{A,1}, \ldots, c_{A,K}]$, $\boldsymbol{c}_B = [c_{B,1}, \ldots, c_{B,K}]$, and $\boldsymbol{\Lambda}_A(0) = \lim_{n\to\infty} \boldsymbol{\Lambda}_{A,n}(0)$ and $\boldsymbol{\Lambda}_B(0) = \lim_{n\to\infty} \boldsymbol{\Lambda}_{B,n}(0)$.

Let us now consider the cyclic correlation detector proposed in [10]. The test statistic of the detector is given by

$$W_n = n\hat{\boldsymbol{r}}_n \hat{\boldsymbol{\Sigma}}_n^{-1} \hat{\boldsymbol{r}}_n^T \quad (33)$$

where $\hat{\boldsymbol{r}}_n$ is a vector of cyclic correlation estimates, $\hat{\boldsymbol{\Sigma}}_n$ is the estimated cyclic covariance matrix, and n is the number of samples.

We formulate the hypotheses as follows

$$H_0: \quad r_k = 0, \text{ for } k = 1, 2, \ldots, 2N,$$
$$H_n: \quad r_{kn} = \gamma/\sqrt{n}, \text{ for } k = 1, 2, \ldots, 2N,$$

where N is the number of different lags the cyclic correlation is estimated at. The real and imaginary parts of the estimated cyclic correlations are stacked to the same vector $\boldsymbol{r}$.

The statistics $\sqrt{n}\hat{\boldsymbol{r}}_n$ with covariances $\sigma_{c,i}\sigma_{c,k}\lambda_{ik}$ satisfy the conditions (i)-(iii) in (25)-(27) since

$$\text{(i)}\quad \mu'_{kn}(0) = \sqrt{n} > 0,$$
$$\text{(ii)}\quad \lim_{n\to\infty} \frac{\mu'_{kn}(0)}{\sqrt{n}\sigma_{kn}(0)} = \frac{1}{\sigma_{c,k}} = c_k > 0,$$
$$\text{(iii)}\quad \mu'_{kn}(r_{kn}) = \mu'_{kn}(0),\ \sigma_{c,kn}(r_{kn}) = \sigma_{c,kn}(0),$$
$$\lambda_{ikn}(r_{kn}) = \lambda_{ikn}(0),$$

for all $k = 1, 2, \ldots, 2N$. The statistic $\sqrt{n}\hat{\boldsymbol{r}}_n$ is asymptotically normal distributed with asymptotic covariance matrix $\boldsymbol{\Sigma}$ thus satisfying also the condition (iv) in (28). The test statistic W_n is asymptotically χ^2_{2N} distributed under the null hypothesis and $\chi^2_{2N}(d)$ distributed under the alternatives where the non-centrality parameter $d = n\gamma^2 \boldsymbol{c}\boldsymbol{\Lambda}^{-1}\boldsymbol{c}^T$ where $\boldsymbol{\Lambda} = \{\lambda_{ik}\}$. That is, it has the same limiting distribution as $n\{\hat{r}_{kn}/\sigma_{c,k}\}\boldsymbol{\Lambda}^{-1}\{\hat{r}_{kn}/\sigma_{c,k}\}^T$.

Let us now consider the spatial sign cyclic correlation detector. We make the following assumptions:

- A.1 The signal $x(t)$ obeys circularly symmetric complex normal distribution under both hypotheses.
- A.2 Signal power does not depend on time, i.e., $s(t) = E[|x(t)|^2] = s$, $\forall t$. Hence, $R(t,\tau) = E[x(t)x^*(t+\tau)] = \sqrt{s(t)s(t+\tau)}\rho_{xx}(t,\tau) = s\rho_{xx}(t,\tau)$ where $\rho_{xx}(t,\tau)$ is the normalized correlation.
- A.3 Under H_0 the correlation for non-zero time lags is zero, i.e., $\rho_{xx}(t,\tau) = 0$, $\forall t$, $\forall \tau \neq 0$.

The normalized spatial sign correlation for circularly symmetric complex normal distributed input is given by (see Appendix A)

$$\begin{aligned}\rho_{yy}(t,\tau) &= E[S(x(t))S(x^*(t+\tau))] \\ &= \frac{\pi}{4}\rho_{xx}(t,\tau)\ {}_2F_1\left(\frac{1}{2}, \frac{1}{2}; 2; |\rho_{xx}(t,\tau)|^2\right).\end{aligned} \quad (34)$$

Next we will calculate the mean of the spatial sign cyclic correlation and its derivative. From (34) it follows that the mean of the spatial sign cyclic correlation $\hat{R}_{S,kn}(\alpha,\tau)$ in (2)

for fixed α and τ is given by

$$\begin{aligned}
&\mu_k(\tilde{r}_k) \\
&= \frac{1}{n}\sum_{t=0}^{n-1}\frac{\pi}{4}\rho_{xx}(t,\tau)\ {}_2F_1\left(\frac{1}{2},\frac{1}{2};2;|\rho_{xx}(t,\tau)|^2\right)e^{-j2\pi\alpha t} \\
&= \frac{1}{n}\sum_{t=0}^{n-1}\frac{\pi}{4}\rho_{xx}(t,\tau) \\
&\quad\cdot\left(1+\frac{\Gamma(2)}{\Gamma^2(\frac{1}{2})}\sum_{k=1}^{\infty}\frac{\Gamma^2(\frac{1}{2}+k)}{\Gamma(2+k)}\frac{|\rho_{xx}(t,\tau)|^{2k}}{k!}\right)e^{-j2\pi\alpha t} \\
&= \frac{\pi}{4}\frac{\tilde{r}_k}{s}+\frac{1}{n}\sum_{t=0}^{n-1}\frac{\pi}{4}\rho_{xx}(t,\tau) \\
&\qquad\cdot\frac{\Gamma(2)}{\Gamma^2(\frac{1}{2})}\sum_{k=1}^{\infty}\frac{\Gamma^2(\frac{1}{2}+k)}{\Gamma(2+k)}\frac{|\rho_{xx}(t,\tau)|^{2k}}{k!}e^{-j2\pi\alpha t},
\end{aligned} \tag{35}$$

where $\tilde{r}_k$ denotes the sum of the corresponding real and imaginary parts of the cyclic correlation, i.e., $\tilde{r}_k$ is a complex variable ($H_0: \tilde{r}_k = 0$ and $H_n: \tilde{r}_{kn} = \gamma/\sqrt{n}(1+j)$, $k = 1, 2, \ldots, N$, and j denotes the imaginary unit). The first term follows from assumption A.2. Note that $\mu_k(0) = 0$ since there is no cyclostationarity present under H_0 and thus the second term in (35) is zero as well.

To calculate the derivative of the mean, we will use the fact that since the correlation of a cyclostationary process is periodic it has a Fourier series representation [22]

$$R(t,\tau) = \sum_{\alpha}\tilde{r}(\alpha,\tau)e^{j2\pi\alpha t} \tag{36}$$

where we have made the dependence of cyclic correlations to α and τ clearly visible.

The derivative of the mean of $\hat{R}_{S,kn}(\alpha,\tau)$ is now given by

$$\begin{aligned}
&\mu_k'(\tilde{r}_k) = \frac{\partial\mu_k(\tilde{r}_k)}{\partial\tilde{r}_k} \\
&= \frac{\pi}{4}\frac{1}{s}+\frac{\pi}{4}\frac{1}{n}\sum_{t=0}^{n-1}e^{-j2\pi\alpha t}\frac{\partial\rho_{xx}(t,\tau)}{\partial\tilde{r}_k} \\
&\quad\cdot\frac{\partial}{\partial\rho_{xx}(t,\tau)}\left(\rho_{xx}(t,\tau)\frac{\Gamma(2)}{\Gamma^2(\frac{1}{2})}\sum_{k=1}^{\infty}\frac{\Gamma^2(\frac{1}{2}+k)}{\Gamma(2+k)}\frac{|\rho_{xx}(t,\tau)|^{2k}}{k!}\right) \\
&= \frac{\pi}{4}\frac{1}{s}+\frac{\pi}{4}\frac{1}{n}\sum_{t=0}^{n-1}\frac{1}{s}\left(1+\sum_{i,i\neq k}\frac{\partial\tilde{r}_i}{\partial\tilde{r}_k}\right)e^{j2\pi\alpha t}\frac{\Gamma(2)}{\Gamma^2(\frac{1}{2})} \\
&\qquad\cdot\sum_{k=1}^{\infty}\frac{\Gamma^2(\frac{1}{2}+k)}{\Gamma(2+k)}\frac{(k+1)|\rho_{xx}(t,\tau)|^{2k}}{k!}e^{-j2\pi\alpha t} \\
&= \frac{\pi}{4}\frac{1}{s}\left(1+\frac{1}{n}\sum_{t=0}^{n-1}\left(\left(1+\sum_{i,i\neq k}\frac{\partial\tilde{r}_i}{\partial\tilde{r}_k}\right)\frac{\Gamma(2)}{\Gamma^2(\frac{1}{2})}\right.\right. \\
&\qquad\left.\left.\cdot\sum_{k=1}^{\infty}\frac{\Gamma^2(\frac{1}{2}+k)}{\Gamma(2+k)}\frac{(k+1)|\rho_{xx}(t,\tau)|^{2k}}{k!}\right)\right),
\end{aligned} \tag{37}$$

where we have used the fact that $\frac{\partial R(t,\tau)}{\partial\tilde{r}_k} = s\frac{\partial\rho_{xx}(t,\tau)}{\partial\tilde{r}_k} = \left(1+\sum_{i,i\neq k}\frac{\partial\tilde{r}_i}{\partial\tilde{r}_k}\right)e^{j2\pi\alpha t}$.

From assumption A.3, it follows that the second term inside the parentheses is zero when $\tilde{r}_k = 0$ and approaches zero as n goes to infinity since $\rho_{xx}(t,\tau) = 0, \forall\tau \neq 0$ under H_0, and since $\lim_{n\to\infty}\tilde{r}_{kn} = \lim_{n\to\infty}\gamma/\sqrt{n}(1+j) = 0$, and thus, $\lim_{n\to\infty}\rho_{xx}(t,\tau) = 0, \forall\tau \neq 0$. Hence, we conclude that $\mu_k'(0) = \frac{\pi}{4}\frac{1}{s}$ and $\lim_{n\to\infty}\mu_k'(\tilde{r}_{kn})/\mu_k'(0) = 1$. That is, the mean function satisfies the conditions (i) and (iii) in (25) and (27), respectively.

The variance of $\hat{R}_{S,kn}$ is given by

$$\begin{aligned}
&\sigma_k^2(\tilde{r}_k) \\
&= \mathrm{Var}\left(\frac{1}{n}\sum_{t=0}^{n-1}S(x(t))S(x^*(t+\tau))e^{-j2\pi\alpha t}\right) \\
&= \frac{1}{n^2}\sum_{t=0}^{n-1}\mathrm{Var}\left(S(x(t))S(x^*(t+\tau))e^{-j2\pi\alpha t}\right) \\
&\quad+\frac{1}{n^2}\sum_{t=0}^{n-1}\sum_{\substack{k=0\\k\neq t}}^{n-1}\mathrm{Cov}\big(S(x(t))S(x^*(t+\tau))e^{-j2\pi\alpha t}, \\
&\qquad\qquad S(x^*(k))S(x(k+\tau))e^{j2\pi\alpha k}\big) \\
&= \frac{1}{n^2}\sum_{t=0}^{n-1}\left(E[|S(x(t))S(x^*(t+\tau))e^{-j2\pi\alpha t}|^2]\right. \\
&\qquad\left.-|E[S(x(t))S(x^*(t+\tau))e^{-j2\pi\alpha t}]|^2\right) \\
&\quad+\frac{1}{n^2}\sum_{t=0}^{n-1}\sum_{\substack{k=0\\k\neq t}}^{n-1}\mathrm{Cov}\big(S(x(t))S(x^*(t+\tau))e^{-j2\pi\alpha t}, \\
&\qquad\qquad S(x^*(k))S(x(k+\tau))e^{j2\pi\alpha k}\big) \\
&= \frac{1}{n}\left(1-\frac{\pi^2}{16}|\rho_{xx}(t,\tau)|^2\ {}_2F_1\left(\frac{1}{2},\frac{1}{2};2;|\rho_{xx}(t,\tau)|^2\right)\right)^2 \\
&\quad+\frac{1}{n}\sum_{t=0}^{n-1}\sum_{\substack{k=0\\k\neq t}}^{n-1}\mathrm{Cov}\big(S(x(t))S(x^*(t+\tau))e^{-j2\pi\alpha t}, \\
&\qquad\qquad S(x^*(k))S(x(k+\tau))e^{j2\pi\alpha k}\big)\Bigg),
\end{aligned} \tag{38}$$

where we have used for the variance the following relation: $\mathrm{Var}(x) = E[|x|^2] - |E[x]|^2$.

Now $\sigma_k^2(0) = 1/n$ and $\lim_{n\to\infty}\sigma_k^2(\tilde{r}_{kn})/\sigma_k^2(0) = 1$ since using assumption A.3 the second and third terms inside the parentheses in (38) approach zero as n goes to infinity. Thus, the variance satisfies the condition (iii) in (27).

Let $\hat{\boldsymbol{r}}_{ss}$ now denote a vector that consists of the real and imaginary parts of the estimated spatial sign cyclic correlation stacked to the same vector, i.e. $\hat{\boldsymbol{r}}_{ss} = [\mathrm{Re}\{\hat{\boldsymbol{r}}_S(\alpha)\}, \mathrm{Im}\{\hat{\boldsymbol{r}}_S(\alpha)\}]$. It follows from the above results that the statistic $\sqrt{n}\hat{\boldsymbol{r}}_{ss}$ satisfies the conditions (i)-(iv) in (25)-(28) with

$$c_{S,k} = \lim_{n\to\infty}\frac{\mu_{S,kn}'(0)}{\sqrt{n}\sigma_{S,kn}(0)\frac{1}{\sqrt{2}}} = \frac{\pi}{4}\frac{1}{\frac{s}{\sqrt{2}}},\ k = 1, 2, \ldots, 2N. \tag{39}$$

Note also that $s = \sqrt{2}\sigma_c$ where σ_c is the standard deviation of the cyclic correlation estimator (assuming that $\sigma_c = \sigma_{c,k}$, $\forall k$). The factor $\sqrt{2}$ comes from the fact that s contains the contribution from both the real and imaginary part.

Now the test statistic $n\hat{\boldsymbol{r}}_{ss}\hat{\boldsymbol{r}}_{ss}^T = n\hat{\boldsymbol{r}}_{ss}\boldsymbol{I}^{-1}\hat{\boldsymbol{r}}_{ss}^T$, where $\boldsymbol{I}$ denotes the identity matrix, is χ^2_{2N} distributed under the null hypothesis and $\chi^2_{2N}(d_S)$ distributed under the alternatives where the non-centrality parameter $d_S = n\gamma^2\frac{\pi^2}{16}\{\frac{1}{\sigma_c}\}\{\frac{1}{\sigma_c}\}^T$.

Finally, the ARE of the spatial sign cyclic correlation detector relative to the cyclic correlation detector for a complex normal input is given by

$$ARE = \frac{\pi^2}{16}\frac{\{\frac{1}{\sigma_c}\}\{\frac{1}{\sigma_c}\}^T}{\{\frac{1}{\sigma_c}\}\boldsymbol{\Lambda}^{-1}\{\frac{1}{\sigma_c}\}^T}. \quad (40)$$

REFERENCES

[1] J. Mitola III and G. Q. Maquire, Jr., "Cognitive Radio: Making Software Radios More Personal," *IEEE Pers. Commun.*, vol. 6, no. 4, pp. 13–18, Aug. 1999.

[2] S. Haykin, "Cognitive Radio: Brain-Empowered Wireless Communications," *IEEE J. Select. Areas Commun.*, vol. 23, no. 2, pp. 201–220, Feb. 2005.

[3] I. F. Akyildiz, W.-Y. Lee, M. C. Vuran, and S. Mohanty, "NeXt Generation/Dynamic Spectrum Access/Cognitive Radio Wireless Networks: A Survey," *Computer Networks*, vol. 50, no. 13, pp. 2127–2159, Sep. 2006.

[4] D. Middleton, "Non-Gaussian noise models in signal processing for telecommunications: New methods and results for Class A and Class B noise models," *IEEE Trans. Inform. Theory*, vol. 45, no. 4, pp. 1129–1149, May 1999.

[5] K. L. Blackard, T. S. Rappaport, and C. W. Bostian, "Measurements and Models of Radio Frequency Impulsive Noise for Indoor Wireless Communications," *IEEE J. Select. Areas Commun.*, vol. 11, no. 7, pp. 991–1001, Sep. 1993.

[6] M. G. Sanchéz, L. de Haro, M. Calvo, A. Mansilla, C. Montero, and D. Oliver, "Impulsive Noise Measurements and Characterization in a UHF Digital TV Channel," *IEEE Trans. Electromagn. Compat.*, vol. 41, no. 2, pp. 124–136, May 1999.

[7] J. Shi, A. Bettner, G. Chinn, K. Slattery, and X. Dong, "A study of platform EMI from LCD panels: Impact on wireless, root causes and mitigation methods, " in *Proc. IEEE Int. Symp. Electromagn. Compat.*, vol. 3, pp. 626–631, Portland, OR, USA, Aug. 14–18, 2006.

[8] M. Nassar, K. Gulati, M. R. DeYoung, B. L. Evans, K. R. Tinsley, "Mitigating near-field interference in laptop embedded wireless transceivers," submitted to *Journal of Signal Processing Systems*, Oct. 2008. Available: http://users.ece.utexas.edu/∼bevans/projects/rfi/ [Accessed May. 13, 2009].

[9] W. A. Gardner, "Signal Interception: A Unifying Theoretical Framework for Feature Detection," *IEEE Trans. Commun.*, vol. 36, no. 8, pp. 897–906, Aug. 1988.

[10] A. V. Dandawaté and G. B. Giannakis, "Statistical Tests for Presence of Cyclostationarity," *IEEE Trans. Signal Process.*, vol. 42, no. 9, pp. 2355–2369, Sep. 1994.

[11] J. Lundén, V. Koivunen, A. Huttunen and H. V. Poor, "Spectrum Sensing in Cognitive Radios Based on Multiple Cyclic Frequencies," in *Proc. 2nd Int. Conf. on Cognitive Radio Oriented Wireless Networks and Communications*, Orlando, FL, USA, Jul. 31–Aug. 3, 2007.

[12] J. Lundén, V. Koivunen, A. Huttunen and H. V. Poor, "Censoring for Collaborative Spectrum Sensing in Cognitive Radios," in *Proc. 41st Asilomar Conf. on Signals, Systems, and Computers*, Pacific Grove, CA, USA, Nov. 4-7, 2007.

[13] T. E. Biedka, L. Mili, and J. H. Reed, "Robust Estimation of Cyclic Correlation in Contaminated Gaussian Noise," in *Proc. 29th Asilomar Conf. on Signals, Systems, and Computers*, vol. 1, Pacific Grove, CA, USA, Oct. 30–Nov. 2, 1995.

[14] L. Izzo, L. Paura, and M. Tanda, "Signal Interception in Non-Gaussian Noise," *IEEE Trans. Commun.*, vol. 40, no. 6, pp. 1030–1037, Jun. 1992.

[15] S. A. Kassam, "Nonparametric Signal Detection," in *Advances in Statistical Signal Processing*, H. V. Poor and J. B. Thomas, Eds., vol. 2, pp. 66–91, JAI Press Inc., 1993.

[16] S. Visuri, V. Koivunen, and H. Oja, "Sign and Rank Covariance Matrices," *J. Statistical Planning and Inference*, vol. 91, no. 2, pp. 557–575, Dec. 2000.

[17] W. A. Gardner, R. S. Roberts, "One-Bit Spectral-Correlation Algorithms," *IEEE Trans. Signal Process.*, vol. 41, no. 1, pp. 423–427, Jan. 1993.

[18] C. Croux, E. Ollila, and H. Oja, "Sign and rank covariance matrices: statistical properties and application to principal components analysis," *Statistical Data Analysis Based on the L1-norm and Related Methods*, Ed. Y. Dodge, pp. 257–271, Basel: Birkhäuser 2002.

[19] C. Cordeiro, K. Challapali, D. Birru, and S. Shankar, "IEEE 802.22: An Introduction to the First Wireless Standard based on Cognitive Radios," *Journal of Communications*, vol. 1, no. 1, pp. 38–47, Apr. 2006.

[20] European Telecommunications Standards Institute, "Digital Video Broadcasting (DVB), Framing structure, channel coding and modulation for digital terrestrial television" ETSI EN 300 744 v1.5.1 (2004-11), Apr. 11, 2004. [Online]. Available: http://pda.etsi.org/pda/queryform.asp [Accessed Apr. 10, 2008].

[21] D. A. S. Fraser, *Nonparametric methods in statistics*, New York: John Wiley & Sons, 1957.

[22] W. A. Gardner, A. Napolitano, and L. Paura, "Cyclostationarity: Half a Century of Research," *Signal Processing*, Vol. 86, pp. 639-697, Apr. 2006.

[23] T. L. Lai, "Sequential Analysis: Some Classical Problems and New Challenges," *Statistica Sinica*, vol. 11, no. 2, pp. 303–408, Apr. 2001.

[24] S. A. Kassam, *Signal Detection in Non-Gaussian Noise*, New York: Springer-Verlag, 1988.

[25] E. J. Hannan, "The Asymptotic Powers of Certain Tests Based on Multiple Correlations," *J. Royal Statistical Society. Series B (Methodological)*, vol. 18, no. 2, pp. 227–233, 1956.

[26] P. Rostaing, E. Thierry, and T. Pitarque, "Asymptotic Performance Analysis of the Single-Cycle Detector," in *Proc. IEEE European Signal Processing Conference (EUSIPCO'96)*, Trieste, Italy, Sep. 10–13, 1996, pp. 671–674.

[27] P. Rostaing, E. Thierry, and T. Pitarque, "Asymptotic Performance Analysis of Cyclic Detectors," *IEEE Trans. Commun.*, vol. 47, no. 1, pp. 10–13, Jan. 1999.

[28] M. Öner and F. Jondral, "Air Interface Identification for Software Radio Systems," *Int. J. Electron. Commun.*, vol. 61, no. 2, pp. 104-117, Feb. 2007.

[29] K. S. Vastola, "Threshold detection in narrow-band non-Gaussian noise," *IEEE Trans. Commun.*, vol. COM-32, no. 2, pp. 134–139, Feb. 1984.

[30] C. L. Nikias and M. Shao, *Signal Processing with Alpha-Stable Distributions and Applications*, New York: John Wiley & Sons, 1995.

[31] I. S. Reed, "On the use of Laguerre Polynomials in Treating the Envelope and Phase Components of Narrow-Band Gaussian Noise," *IRE Trans. Inform. Theory*, vol. IT–5, pp. 102–105, Sep. 1959.

[32] G. Jacovitti and A. Neri, "Estimation of the Autocorrelation Function of Complex Gaussian Stationary Processes by Amplitude Clipped Signals," *IEEE Trans. Inform. Theory*, vol. 40, no. 1, pp. 239–245, Jan. 1994.

Jarmo Lundén (S'04) received the M.Sc. (Tech) degree with distinction in communications engineering from the Department of Electrical and Communications Engineering, Helsinki University of Technology, Espoo, Finland, in 2005, where he is currently pursuing the D.Sc. (Tech) degree. From September 2007 to March 2008, he was a visiting researcher at the University of Pennsylvania, Philadelphia, USA.

His research interests include spectrum sensing for cognitive radio as well as radar signal interception and identification.

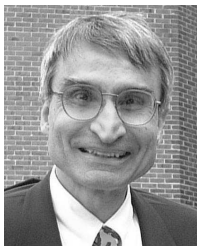

Saleem A. Kassam is the *Solomon and Sylvia Charp Professor of Electrical Engineering* at the Department of Electrical and Systems Engineering, University of Pennsylvania, Philadelphia, PA, where he has been on the faculty since 1975. He received the B.S. degree from Swarthmore College, Swarthmore, PA, in 1972, and the Ph.D. degree in Electrical Engineering from Princeton University, Princeton, NJ, in 1975. From 1992 to 1994 he was Chairman of the Department of Electrical Engineering at the University of Pennsylvania.

He is a member of Phi Beta Kappa, a Fellow of the IEEE, and has served on the Board of Governors of the IEEE Information Theory Society. He is the author of *Signal Detection in Non-Gaussian Noise* (Springer-Verlag, 1988).

His research interests are in the areas of statistical signal processing and communication theory, with interests in high resolution imaging systems, adaptive systems, signal detection and estimation, and blind equalization and source separation.

Visa Koivunen (Senior Member, IEEE) received his D.Sc. (EE) degree with honors from the University of Oulu, Dept. of Electrical Engineering. He received the primus doctor (best graduate) award among the doctoral graduates in years 1989-1994. From 1992 to 1995 he was a visiting researcher at the University of Pennsylvania, Philadelphia, USA. From August 1997 to August 1999 he was an Associate Professor at the Signal Processing Laboratory, Tampere University of Technology. Since 1999 he has been a Professor of Signal Processing at the Department of Electrical and Communications Engineering, Helsinki University of Technology (HUT), Finland. He is one of the Principal Investigators in SMARAD (Smart Radios and Wireless Systems) Center of Excellence in Radio and Communications Engineering nominated by the Academy of Finland. He has been also adjunct full professor at the University of Pennsylvania, Philadelphia, USA. During his sabbatical leave in 2006-2007 he was Visiting Fellow at Nokia Research Center as well as visiting fellow at Princeton University.

Dr. Koivunen's research interest include statistical, communications and sensor array signal processing. He has published more than 270 papers in international scientific conferences and journals. He co-authored the papers receiving the best paper award in IEEE PIMRC 2005, EUSIPCO 2006 and EuCAP 2006. He has been awarded the IEEE Signal Processing Society best paper award for the year 2007 (co-authored with J. Eriksson). He served as an associate editor for IEEE Signal Processing Letters. He is a member of the editorial board for the Signal Processing journal and Journal of Wireless Communication and Networking. He is also a member of the IEEE Signal Processing for Communication (SPCOM-TC) and Sensor Array and Multichannel (SAM-TC) Technical Committees. He was the general chair of the IEEE SPAWC (Signal Processing Advances in Wireless Communication) 2007 conference in Helsinki, June 2007.